Supplemental Material

Data S1. Supplemental Discussion

To evaluate a role of mTORC1 in compensatory fetal cardiac growth we investigated the effect of prenatal rapamycin treatment on *cHccs*$^{+/-}$ mice. The latter develop a tissue mosaic of healthy and defective cells in the ventricular myocardium at mid-gestation, but compensatory hyperproliferation of healthy cells allows formation of a fully functional heart primarily composed of healthy cardiomyocytes at birth.[1] Nevertheless, embryonic heart regeneration is insufficient to completely build up the heart, such that neonatal *cHccs*$^{+/-}$ mice exhibit reduced heart size at birth due to a reduced number of cardiomyocytes.[2] The latter is postnatally compensated for by accelerated physiological hypertrophy, resulting in normalization of organ size by early adulthood.[2] Here we show increased phosphorylation of the mTORC1 downstream targets S6K1 and S6 ribosomal protein in neonatal *cHccs*$^{+/-}$ hearts compared to littermate controls (Figure 4), suggesting a role of mTORC1 in pre- or postnatal compensatory growth and adaptation. Surprisingly, prenatal rapamycin treatment causes only marginal differences in *cHccs*$^{+/-}$ compared to *Hccs*$^{+/+}$ newborn hearts. mTORC1 does not seem to be specifically required for establishing the size of *cHccs*$^{+/-}$ hearts by birth, given that the reduction in heart weight in rapamycin compared to vehicle treated animals is similar to *Hccs*$^{+/+}$ mice (34.5% versus 35.3%). Also, the previously reported reduction in heart weight and HW/BW ratio in *cHccs*$^{+/-}$ compared to *Hccs*$^{+/+}$ hearts at birth [2] was evident in vehicle and rapamycin treated animals but not further aggravated by rapamycin. Prenatal rapamycin treatment does not specifically impair proliferation in neonatal *cHccs*$^{+/-}$ hearts. Of note, compensatory proliferation in *cHccs*$^{+/-}$ hearts is no longer evident at P1, as reported previously [2] and observed in vehicle treated *cHccs*$^{+/-}$ compared to *Hccs*$^{+/+}$ neonates. A limitation of our studies in this regard is that we did not determine proliferation specifically in healthy versus HCCS deficient cardiomyocytes or non-myocytes. Therefore, slightly different proliferation rates in one cell population versus the other, which might be differentially affected by rapamycin in *cHccs*$^{+/-}$ compared to *Hccs*$^{+/+}$ neonates, would be missed. Nevertheless, hyperproliferation of healthy cardiomyocytes in *cHccs*$^{+/-}$ hearts was mainly observed during embryonic stages (i.e. at 11.5 and 13.5 dpc).[1] Consequently, the rapamycin treatment protocol applied in the current study (i.e. starting at 15.5 dpc) misses the main window of compensatory proliferation. Commencement of rapamycin treatment at 11.5 dpc, however, resulted in spontaneous abortions and fetal death, thereby impeding attempts to study the role of mTORC1 in the main regenerative phase. Proliferation during the fetal period was not investigated in our previous [1] or the current study, such that a potential effect of rapamycin treatment on compensatory proliferation of healthy cardiomyocytes in the fetal *cHccs*$^{+/-}$ heart cannot be excluded. Such scenario seems unlikely, however, given that the reduction in heart weight and HW/BW ratio in *cHccs*$^{+/-}$ compared to *Hccs*$^{+/+}$ neonates is not aggravated by rapamycin. In summary, future studies using adapted rapamycin treatment protocols or genetic models resulting in heart specific inhibition of mTORC1 might help to unravel its precise role in embryonic heart regeneration.

Whereas apoptosis rates in the neonatal heart are not different in *cHccs*$^{+/-}$ compared to *Hccs*$^{+/+}$ mice under baseline conditions (see [2] and vehicle groups in the current study), prenatal rapamycin treatment induces cell death in both genotypes when compared to vehicle and apoptosis is even further increased in rapamycin treated *cHccs*$^{+/-}$ hearts. It is tempting to speculate that the latter might be caused by death of the ~10% of HCCS deficient cardiomyocytes that remain in the neonatal *cHccs*$^{+/-}$ heart.[1] Although we did not differentiate between cell types (i.e. cardiomyocytes versus non-myocytes or healthy versus HCCS deficient cardiomyocytes) when performing TUNEL staining, immunofluorescence staining for cleaved caspase 3 did not reveal increased apoptosis of HCCS deficient cardiomyocytes upon rapamycin treatment (data not shown). Thus, the primary cell type undergoing cell

death in the neonatal *Hccs*$^{+/+}$ as well as *cHccs*$^{+/-}$ heart upon mTORC1 inhibition will have to be determined in future studies.

Prenatal rapamycin treatment more severely disturbs fetal cardiomyocyte growth in *cHccs*$^{+/-}$ versus *Hccs*$^{+/+}$ mice compared to their respective vehicle group. Whereas cardiomyocyte cross sectional area is not different between genotypes under baseline conditions (see [2] and vehicle treated animals), rapamycin causes a significant reduction in *cHccs*$^{+/-}$ compared to *Hccs*$^{+/+}$ mice. These data suggest that establishing a normal cardiomyocyte size in the neonatal *cHccs*$^{+/-}$ heart depends on mTORC1. In contrast, hyperactivation of mTORC1 is unable to raise cell size above the level of control mice to compensate for the reduced cardiomyocyte number and normalize organ size at birth. This suggests that plasticity of cardiomyocyte size in the perinatal heart is limited and compensatory hypertrophic growth primarily occurs during postnatal development, as observed in *cHccs*$^{+/-}$ mice.[2] Another possible explanation is that further increasing cardiomyocyte size might shift physiological hypertrophy towards pathological cardiac growth and maladaptive remodeling. Therefore, cardiomyocyte size appears to be tightly controlled in the neonatal heart even under conditions of reduced cell number, and mTORC1 activity might be restricted to prevent unrestrained cardiac growth. An important question in this regard is, why the reduced CSA in *cHccs*$^{+/-}$ compared to *Hccs*$^{+/+}$ neonates upon rapamycin treatment does not translate into a more pronounced reduction in *cHccs*$^{+/-}$ heart size. The latter could be due to compensation by increased extracellular matrix deposition (i.e. fibrosis). Although we did not measure fibrosis in the neonatal heart, we did not detect differences between rapamycin and vehicle treated mice or between genotypes in adulthood, making a transient fibrotic compensation in rapamycin treated *cHccs*$^{+/-}$ hearts around birth rather unlikely. In addition, myocardial replacement fibrosis is rarely observed in newborn mice and the neonatal murine heart can fully regenerate after apex resection or myocardial infarction without formation of a permanent fibrotic scar.[3] Another possible explanation for maintained heart size in rapamycin treated *cHccs*$^{+/-}$ relative to *Hccs*$^{+/+}$ neonates despite reduced cardiomyocyte size would be compensation by a non-myocyte cell population. In this regard, adult *Hccs*$^{+/+}$ hearts show a slightly reduced cardiomyocyte area fraction after prenatal rapamycin compared to vehicle treatment. In the absence of myocardial fibrosis (as demonstrated in Figure S6), this might indicate an increased abundance of a non-myocyte cell population. Whether changes in cardiomyocyte area fraction in rapamycin treated hearts are already detectable at birth and more pronounced in *cHccs*$^{+/-}$ neonates is uncertain, however. In summary, future studies will have to investigate possible changes in myocardial tissue composition after prenatal rapamycin treatment at birth and in adulthood.

Finally, prenatal rapamycin treatment does not cause any long-term negative effects on cardiac organ size, morphology or LV function in adult *cHccs*$^{+/-}$ compared to *Hccs*$^{+/+}$ mice. Postnatal normalization of heart weight and cardiac output compared to vehicle treated mice is similar in both genotypes. Thus, any effect of prenatal mTORC1 inhibition specifically in *cHccs*$^{+/-}$ hearts can be compensated until early adulthood under baseline conditions. It would be interesting, however, to evaluate whether this still holds true if the heart is challenged by pressure overload, neurohumoral stimulation or ischemia. Furthermore, after prenatal rapamycin treatment mTORC1 activity is restored at postnatal day 3. Thus, postnatal compensatory growth is ... the precise role of mTORC1 in this process cannot be assessed ... still considerable at postnatal day

10.[13] Our previous study has shown normalization of heart size by P3, ... cardiomyocyte hypertrophy in *cHccs*$^{+/-}$ mice by the age of 10 weeks, whereas hearts require extension of the similar period throughout postnatal development.

Supplemental Tables

	n	LV mass (mg)	HW/BW (mg/g)	IVS dia (mm)	LVPW dia (mm)	IVS sys (mm)	LVPW sys (mm)	LVID dia (mm)	LVID sys (mm)	FS (%)	EF (%)	Stroke volume (µl)	Heart rate (bpm)	Cardiac output (ml/min)
V														
***Hccs*$^{+/+}$**	7	5.54 ±0.39	1.21 ±0.04	0.27 ±0.01	0.27 ±0.02	0.43 ±0.02	0.44 ±0.02	1.50 ±0.04	1.02 ±0.04	31.86 ±1.46	63.05 ±1.92	1.29 ±0.09	395.71 ±33.64	0.49 ±0.03
c*Hccs*$^{+/-}$	6	4.81 ±0.37	1.19 ±0.05	0.26 ±0.01	0.27 ±0.01	0.40 ±0.02	0.40 ±0.02	1.41 ±0.05	0.97 ±0.04	31.08 ±1.42	64.06 ±1.98	1.04 ±0.24	383.5 ±30.53	0.37 ±0.07
R														
***Hccs*$^{+/+}$**	6	3.67§§ ±0.21	0.97 ±0.01	0.24 ±0.01	0.26 ±0.01	0.36§ ±0.01	0.38 ±0.02	1.27§§ ±0.05	0.90 ±0.05	29.50 ±1.65	61.38 ±3.00	0.92 ±0.10	340.83 ±27.84	0.32 ±0.05
c*Hccs*$^{+/-}$	7	3.36$^{\#}$ ±0.33	1.08 ±0.04	0.23 ±0.02	0.23 ±0.02	0.34 ±0.02	0.35 ±0.02	1.27 ±0.04	0.92 ±0.23	27.36 ±1.53	55.60$^{\#}$ ±1.77	0.78 ±0.09	359.86 ±29.10	0.29 ±0.04

Table S1. Echocardiographic measurements in neonatal mice after prenatal mTORC1 inhibition

Echocardiography was performed on postnatal day 1 in *Hccs*$^{+/+}$ and c*Hccs*$^{+/-}$ mice after prenatal rapamycin or vehicle treatment. Left ventricular (LV) wall thickness and diameter were determined in end-diastole (dia) and end-systole (sys) and LV mass, contractility and output were calculated ($^{§}p$<0.05 vs. vehicle *Hccs*$^{+/+}$, $^{§§}p$<0.01 vs. vehicle *Hccs*$^{+/+}$, $^{\#}p$<0.05 vs. vehicle c*Hccs*$^{+/-}$). (EF: ejection fraction, FS: fractional shortening, IVS: interventricular septum, LVID: left ventricular internal diameter, LVPW: left ventricular posterior wall, R: rapamycin, V: vehicle)

	n	BW (g)	TL (mm)	LW (mg)	LW/BW (mg/g)	LW/TL (mg/mm)	KW (mg)	KW/BW (mg/g)	KW/TL (mg/mm)	SW (mg)	SW/BW (mg/g)	SW/TL (mg/mm)
V												
***Hccs*$^{+/+}$**	8	17.12 ±0.56	15.13 ±0.14	771.36 ±52.95	44.79 ±1.81	50.83 ±3.02	111.86 ±3.99	6.55 ±0.20	7.39 ±0.22	43.40 ±4.97	2.50 ±0.23	2.85 ±0.31
c*Hccs*$^{+/-}$	6	18.67 ±0.57	15.50 ±0.13	893.38 ±41.41	47.86 ±1.76	57.61 ±2.51	114.98 ±3.25	6.18 ±0.20	7.42 ±0.21	41.17 ±5.29	2.18 ±0.24	2.65 ±0.33
R												
***Hccs*$^{+/+}$**	9	15.26§ ±0.51	14.39§§ ±0.14	713.27 ±30.16	46.65 ±0.75	49.52 ±1.90	96.99 ±4.02	6.36 ±0.15	6.73 ±0.23	37.70 ±3.92	2.45 ±0.21	2.62 ±0.27
c*Hccs*$^{+/-}$	6	15.78$^{\#}$ ±1.08	14.82 ±0.35	703.93 ±60.75	44.38 ±1.63	47.22 ±3.27	97.98 ±5.66	6.24 ±0.11	6.59 ±0.24	28.67 ±5.65	1.73 ±0.24	1.90 ±0.34

Table S2. Body and organ weights in adult mice after prenatal rapamycin or vehicle treatment.

Body and organ weights were determined in 11 week old *Hccs*$^{+/+}$ and c*Hccs*$^{+/-}$ mice after prenatal rapamycin or vehicle treatment ($^{\S}p<0.05$ vs. vehicle *Hccs*$^{+/+}$, $^{\S\S}p<0.01$ vs. vehicle *Hccs*$^{+/+}$, $^{\#}p<0.05$ vs. vehicle c*Hccs*$^{+/-}$). (BW: body weight, KW: kidney weight, LW: liver weight, SW: spleen weight, TL: tibia length, R: rapamycin, V: vehicle)

	n	LV mass (mg)	HW/BW (mg/g)	IVS dia (mm)	LVPW dia (mm)	IVS sys (mm)	LVPW sys (mm)	LVID dia (mm)	LVID sys (mm)	FS (%)	EF (%)	Stroke volume (µl)	Heart rate (bpm)	Cardiac output (ml/min)
V														
***Hccs*$^{+/+}$**	7	92.14 ±4.18	5.16 ±0.26	0.74 ±0.02	0.75 ±0.02	0.99 ±0.02	0.94 ±0.05	3.66 ±0.11	2.87 ±0.12	21.66 ±1.53	43.64 ±2.38	18.19 ±1.68	429.29 ±5.97	7.82 ±0.75
c*Hccs*$^{+/-}$	6	107.42 ±7.68	5.86 ±0.38	0.76 ±0.06	0.76 ±0.04	0.99 ±0.05	0.98 ±0.06	3.96 ±0.18	3.07 ±0.24	23.07 ±2.81	45.18 ±4.64	15.75 ±2.06	412.50 ±12.94	6.55 ±0.99
R														
***Hccs*$^{+/+}$**	9	70.93 ±5.06	4.51 ±0.23	0.62 ±0.04	0.61 ±0.04	0.83 ±0.06	0.83 ±0.05	3.64 ±0.08	2.84 ±0.14	22.21 ±2.37	45.71 ±3.70	16.97 ±1.19	404.89 ±21.28	6.88 ±0.61
c*Hccs*$^{+/-}$	6	84.00 ±9.53	5.13 ±0.29	0.63 ±0.04	0.63 ±0.04	0.88 ±0.08	0.88 ±0.05	3.91 ±0.13	3.00 ±0.19	23.58 ±2.45	47.17 ±4.12	19.26 ±2.23	372.00 ±20.31	7.11 ±0.82

Table S3. Echocardiographic measurements in adult mice after prenatal mTORC1 inhibition.

Echocardiography was performed in 11 week old *Hccs*$^{+/+}$ and c*Hccs*$^{+/-}$ mice after prenatal rapamycin or vehicle treatment. Left ventricular (LV) wall thickness and diameter were determined in end-diastole (dia) and end-systole (sys) and LV mass, contractility and output were calculated. (EF: ejection fraction, FS: fractional shortening, IVS: interventricular septum, LVID: left ventricular internal diameter, LVPW: left ventricular posterior wall, R: rapamycin, V: vehicle)

Supplemental Figures

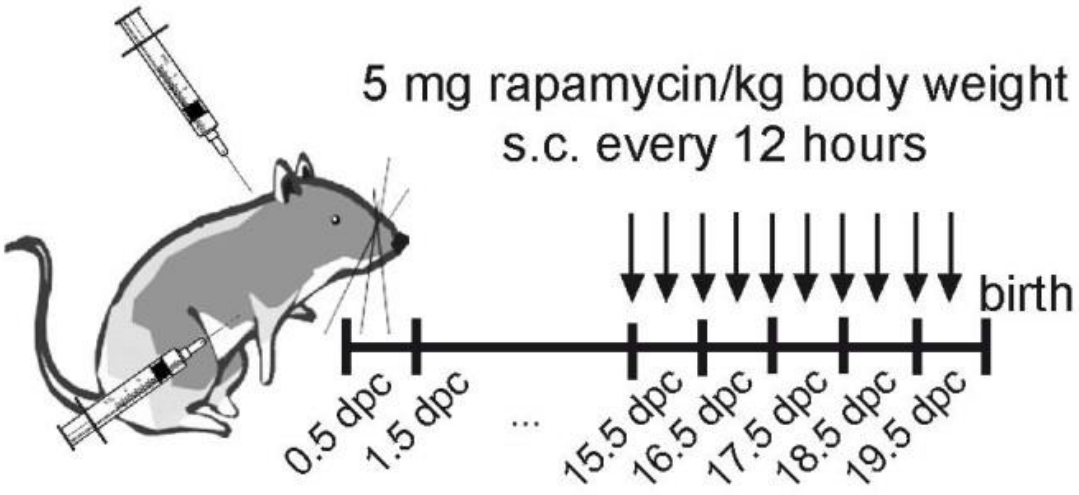

Figure S1. Inhibition of mTORC1 in fetal and neonatal mice by rapamycin treatment of pregnant dams. Rapamycin was injected subcutaneously at a dose of 5 mg per kg body weight in pregnant dams every 12 h from 15.5 dpc until delivery. As controls, pregnant dams were injected with vehicle only.

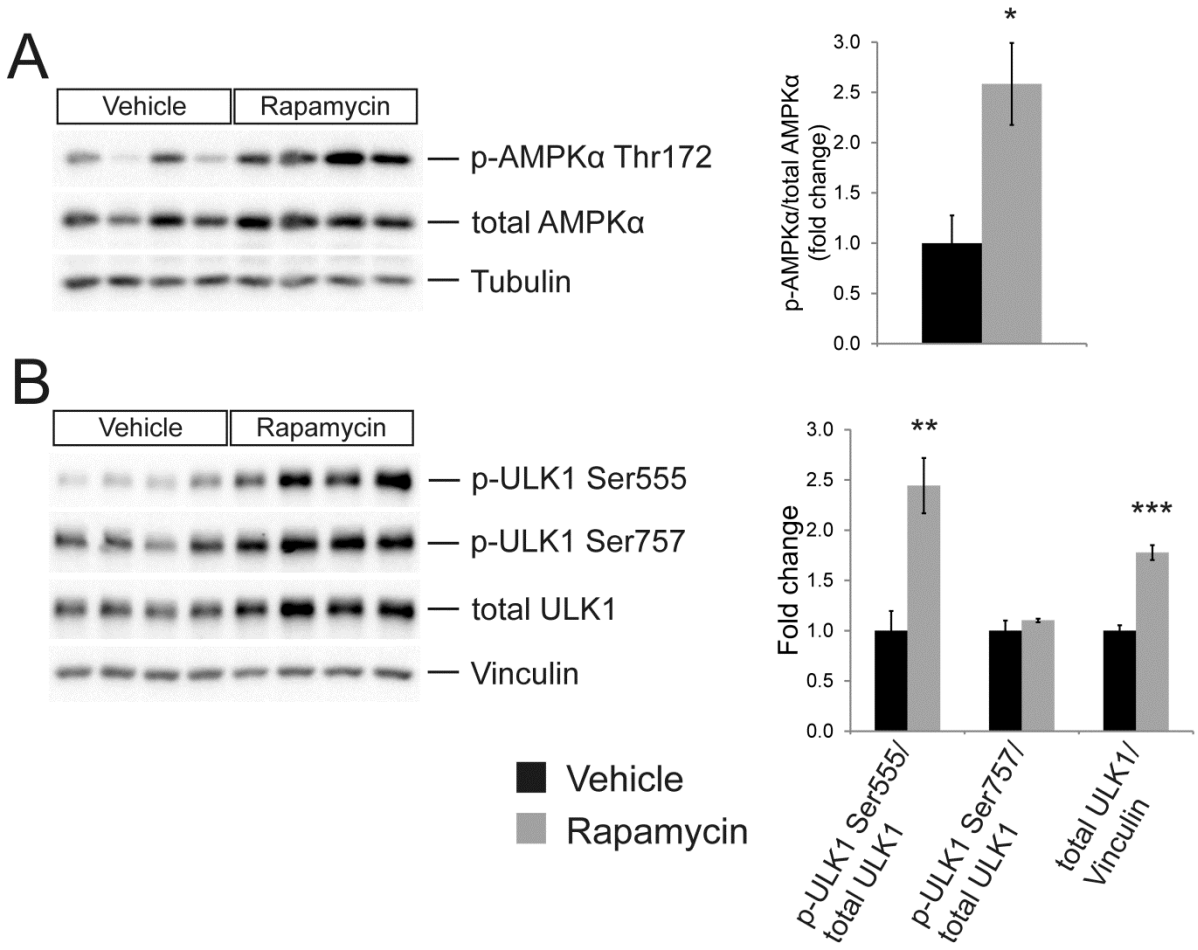

Figure S2. Evaluation of the autophagy regulating kinases AMPK and ULK1 in neonatal hearts after prenatal rapamycin treatment. (A) Phosphorylation of the AMPK (AMP-activated protein kinase) subunit α is increased in neonatal hearts after prenatal rapamycin treatment, indicating AMPK activation. (B) The kinase ULK1 (Unc-51 like autophagy activating kinase 1) is phosphorylated by AMPK at Ser555 to initiate autophagy whereas mTOR phosphorylates ULK1 at Ser757 to inhibit autophagy. Consistent with AMPK activation ULK1 Ser555 phosphorylation is increased in neonatal hearts after prenatal rapamycin treatment, whereas Ser757 phosphorylation is unchanged when normalized to total ULK1. Note that the latter is confounded by a significant increase in total ULK1 protein levels in rapamycin compared to vehicle treated hearts. (densitometric quantification n=4 per group in (A) and (B), *p<0.05, **p<0.01, ***p<0.001)

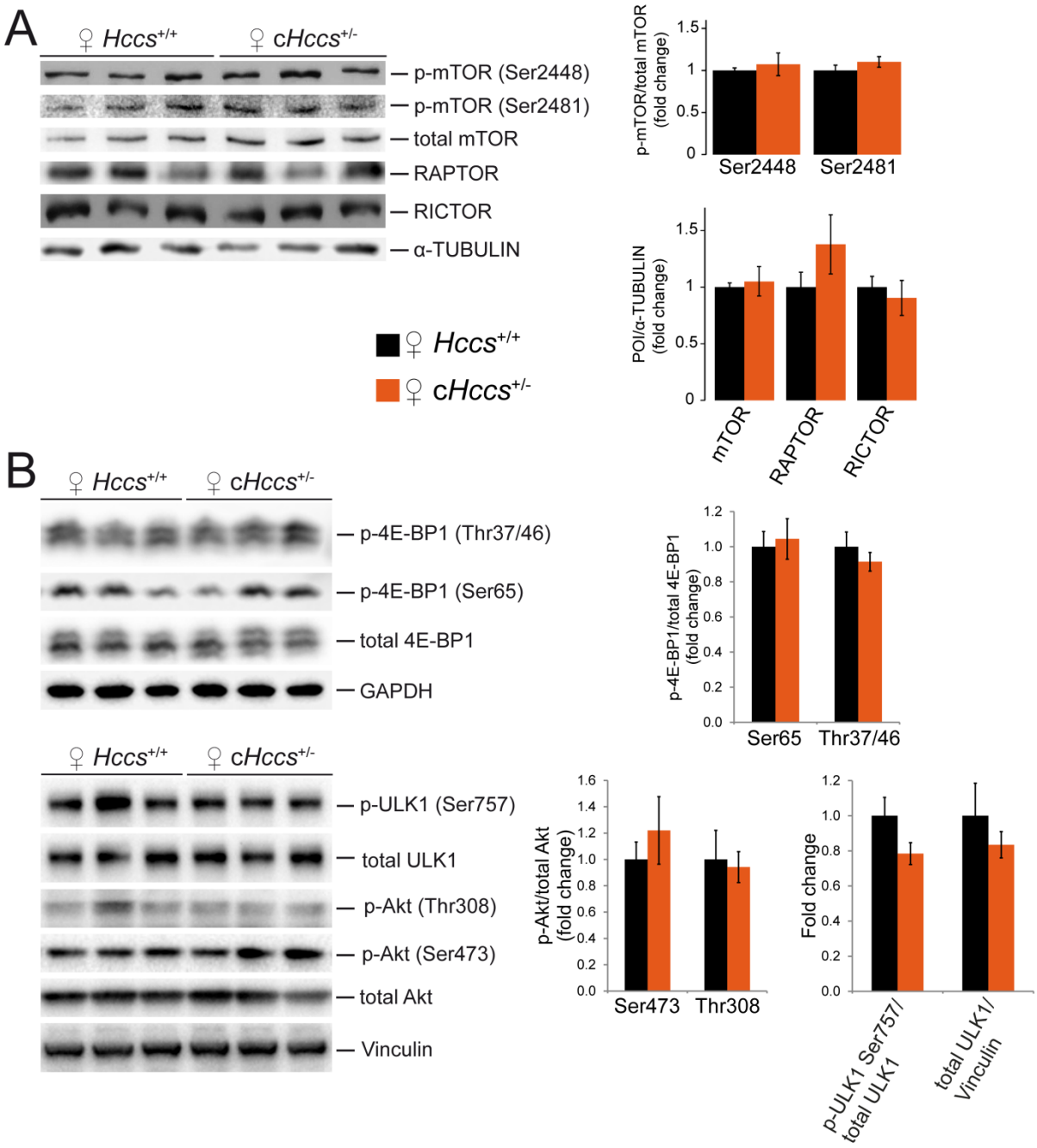

Figure S3. Unaltered phosphorylation of mTOR, ULK1, 4E-BP1 and Akt in neonatal *cHccs*$^{+/-}$ hearts. (A) Phosphorylation of mTOR at Ser2448 and Ser2481 is unaltered in neonatal *cHccs*$^{+/-}$ hearts compared to controls. Similarly, no difference in total protein amounts of mTOR or its interacting proteins RAPTOR or RICTOR (specific for mTOR complex 1 and 2, respectively) is detected between groups (densitometric quantification n=8 per genotype; POI = protein of interest). (B) Phosphorylation of the mTORC1 downstream targets 4E-BP1 and ULK1 (at the mTORC1 dependent site Ser757) is not different between neonatal *cHccs*$^{+/-}$ and control hearts. The kinase Akt acts as both an upstream regulator of mTORC1 as well as mTORC2 downstream target. Phosphorylation of Akt at Thr308 (via the PI3K pathway) and Ser473 (by mTORC2) is unaltered in *cHccs*$^{+/-}$ hearts (densitometric quantification n=5-6 per genotype).

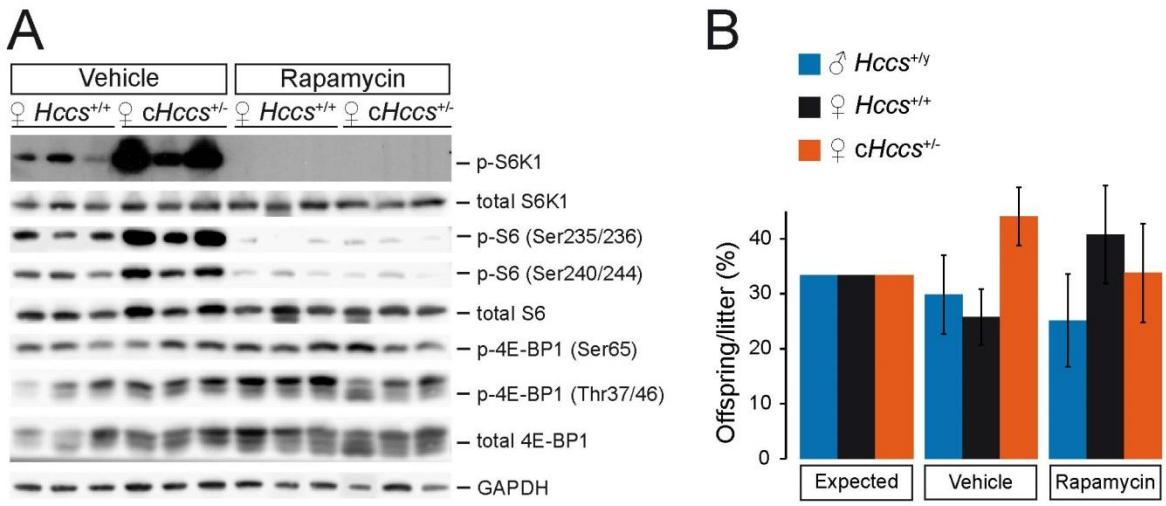

Figure S4. Prenatal mTORC1 inhibition in *cHccs*$^{+/-}$ fetuses does not cause lethality prior to birth. (A) Western blots of heart protein extracts from neonatal (P1) *cHccs*$^{+/-}$ females and their *Hccs*$^{+/+}$ female littermate controls after prenatal vehicle or rapamycin treatment illustrating phosphorylation status of the mTORC1 downstream targets S6K1, S6 and 4E-BP1. Note increased mTORC1 activity towards S6K1 and S6 in *cHccs*$^{+/-}$ females in vehicle treated animals (see main text and Figure 4) but similar reduction of S6K1 and S6 phosphorylation in hearts of rapamycin compared to vehicle treated offspring, indicating successful mTORC1 inhibition in *cHccs*$^{+/-}$ hearts. Phosphorylation of 4E-BP1 was demonstrated to be unaffected by prenatal rapamycin treatment (see main text and Figure 1). (B) Genotype distribution within vehicle as well as rapamycin treated litters was not significantly different from expected genotype frequencies, indicating that *cHccs*$^{+/-}$ females do not exhibit prenatal lethality due to mTORC1 inhibition. Statistical significance between treatment groups and the expected genotype distribution was assessed by *chi*-square test. Statistical significance comparing the frequencies of each genotype between vehicle and rapamycin treated litters was assessed by unpaired 2-tailed Student *t*-tests (n=9 litters per group).

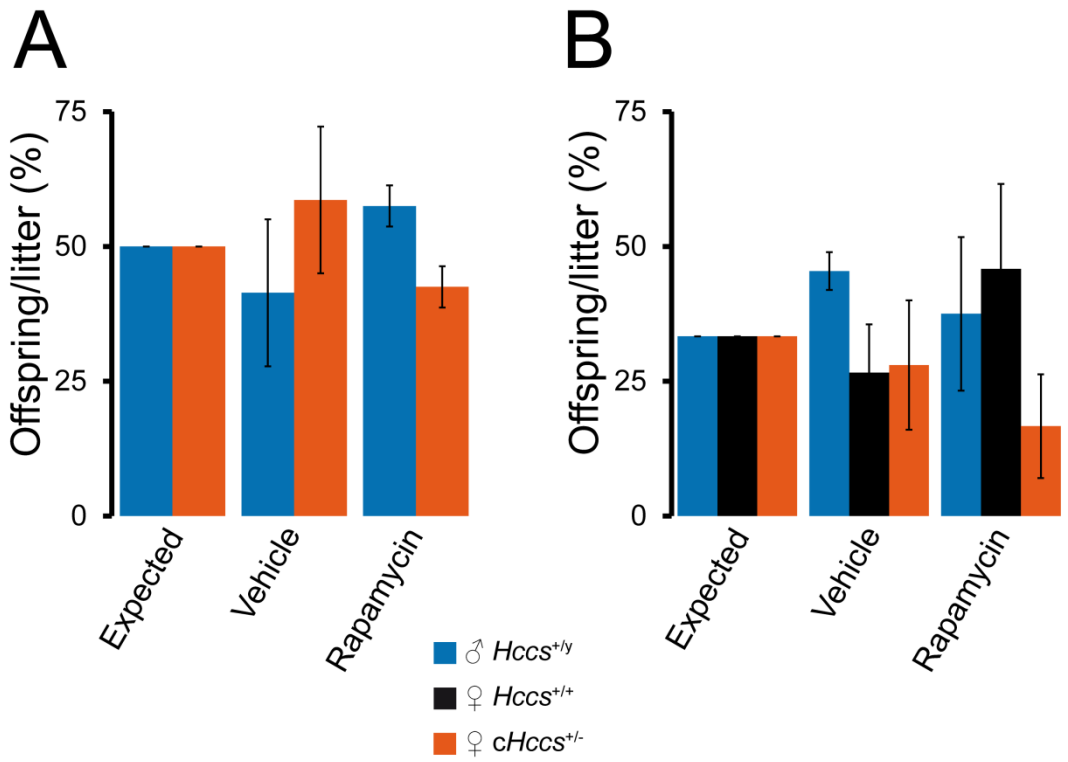

Figure S5. No preferential death of rapamycin treated *cHccs*$^{+/-}$ females after birth. (A) Breeding of males hemizygous for the "floxed" *Hccs* allele (*Hccs*$^{floxed/y}$/*Nkx2.5*$^{+/+}$) to females homozygous for the *Nkx2.5Cre* allele (*Hccs*$^{+/+}$/*Nkx2.5*$^{Cre/Cre}$) generates two possible offspring genotypes, i.e. control males (*Hccs*$^{+/y}$/*Nkx2.5*$^{Cre/+}$) and heterozygous heart conditional *Hccs* knockout females (*Hccs*$^{floxed/+}$/*Nkx2.5*$^{Cre/+}$) at an expected ratio of 50:50. (B) Breeding of males homozygous for the *Nkx2.5Cre* allele (*Hccs*$^{+/y}$/*Nkx2.5*$^{Cre/Cre}$) to females heterozygous for the "floxed" *Hccs* allele (*Hccs*$^{floxed/+}$/*Nkx2.5*$^{+/+}$) generates three postnatally viable genotypes, i.e. control males (*Hccs*$^{+/y}$/*Nkx2.5*$^{Cre/+}$), control females (*Hccs*$^{+/+}$/*Nkx2.5*$^{Cre/+}$) and heterozygous heart conditional *Hccs* knockout females (*Hccs*$^{floxed/+}$/*Nkx2.5*$^{Cre/+}$) at an expected ratio of 33% each. Hemizygous heart conditional *Hccs* knockout males (*Hccs*$^{floxed/y}$/*Nkx2.5*$^{Cre/+}$) die in utero at stage 10.5 dpc.[11] Genotype distribution within vehicle as well as rapamycin treated litters was evaluated at weaning (i.e. at 21 days of age). For both breeding schemes no significant difference compared to expected genotype frequencies was observed, indicating that rapamycin treated *cHccs*$^{+/-}$ females do not preferentially die within the first 12 days after birth (see Figure 6A). Statistical significance between treatment groups and the expected genotype distribution was assessed by *chi*-square test (3 litters per group in (A); 5 vehicle and 4 rapamycin treated litters in (B)).

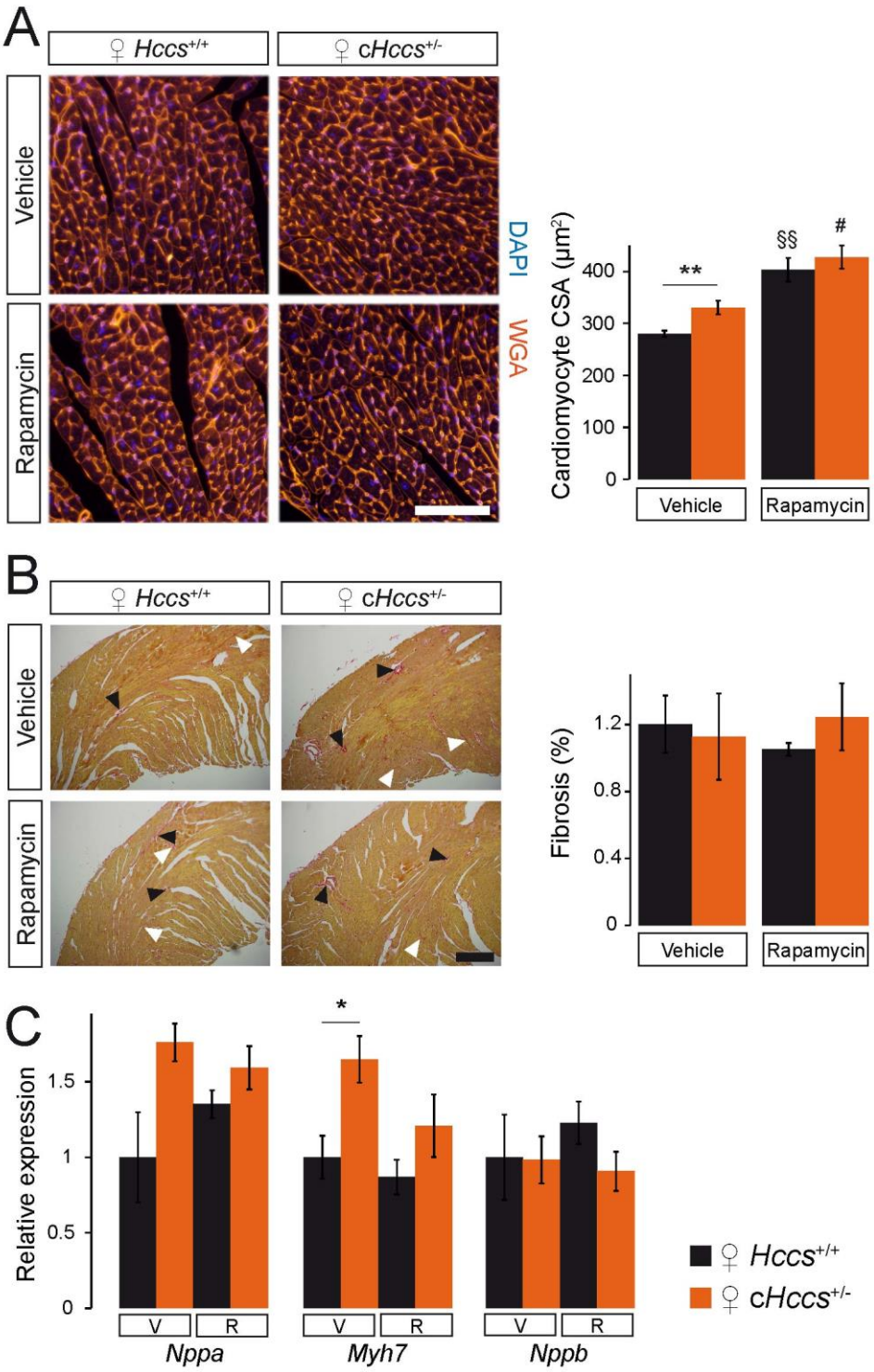

Figure S6. Prenatal mTORC1 inhibition does not cause significantly different tissue remodeling in adult *cHccs*$^{+/-}$ compared to *Hccs*$^{+/+}$ hearts. (A) Fluorescence images of cross-sectioned cardiomyocytes within the left ventricular (LV) myocardium of adult hearts. Cardiomyocyte membranes were stained in red with wheat germ agglutinin (WGA) and nuclei in blue with DAPI (scale bar = 100 µm). Cardiomyocyte cross sectional area (CSA) was significantly larger in *Hccs*$^{+/+}$ as well as *cHccs*$^{+/-}$ hearts exposed to prenatal rapamycin compared to vehicle treatment. Note that compensatory cardiomyocyte hypertrophy in c*Hccs*$^{+/-}$ mice reported previously [12] is evident in the vehicle group but lost in rapamycin

treated hearts (vehicle *Hccs*$^{+/+}$ n=6, rapamycin *Hccs*$^{+/+}$ n=7, vehicle and rapamycin c*Hccs*$^{+/-}$ n=5). (B) Representative images of Sirius Red stained LV myocardium of adult mice. White arrowheads highlight interstitial fibrosis whereas black arrowheads indicate perivascular fibrosis, which was excluded from quantification (scale bar = 300 µm). The contribution of fibrotic tissue to the LV myocardium of adult mice did not reveal differences between treatment groups or genotypes (n=6 for all groups, except vehicle c*Hccs*$^{+/-}$ n=8). (C) Relative *Nppa*, *Myh7* and *Nppb* RNA expression in adult hearts was determined using qRT-PCR to evaluate pathological conditions. No major changes in gene expression were observed in rapamycin (R) compared to vehicle (V) groups in either *Hccs*$^{+/+}$ or *cHccs*$^{+/-}$ hearts (n=8 per group). Note that data used for *Hccs*$^{+/+}$ animals in (A) – (C) are the same as depicted in Figure 8. (**p*<0.05, ***p*<0.01, §§*p*<0.01 vs. vehicle *Hccs*$^{+/+}$, $^{\#}$*p*<0.05 vs. vehicle c*Hccs*$^{+/-}$).

Supplemental References:

1. Drenckhahn JD, Schwarz QP, Gray S, Laskowski A, Kiriazis H, Ming Z, Harvey RP, Du XJ, Thorburn DR, Cox TC. Compensatory growth of healthy cardiac cells in the presence of diseased cells restores tissue homeostasis during heart development. *Dev Cell*. 2008;15:521-533.

2. Drenckhahn JD, Strasen J, Heinecke K, Langner P, Yin KV, Skole F, Hennig M, Spallek B, Fischer R, Blaschke F, Heuser A, Cox TC, Black MJ, Thierfelder L. Impaired myocardial development resulting in neonatal cardiac hypoplasia alters postnatal growth and stress response in the heart. *Cardiovasc Res.* 2015;106:43-54.

3. Foglia MJ, Poss KD. Building and re-building the heart by cardiomyocyte proliferation. *Development.* 2016;143:729-740.